CCR5 Inhibition Prevents Cardiac Dysfunction in the SIV/Macaque Model of HIV

Kathleen M. Kelly, DVM, PhD; Carlo G. Tocchetti, MD, PhD; Alexey Lyashkov, PhD; Patrick M. Tarwater, PhD; Djahida Bedja, MS; David R. Graham, PhD; Sarah E. Beck, DVM; Kelly A. Metcalf Pate, DVM, PhD; Suzanne E. Queen, MS; Robert J. Adams, DVM; Nazareno Paolocci, MD, PhD; Joseph L. Mankowski, DVM, PhD

Background—Diastolic dysfunction is a highly prevalent cardiac abnormality in asymptomatic as well as ART-treated human immunodeficiency virus (HIV) patients. Although the mechanisms underlying depressed cardiac function remain obscure, diastolic dysfunction in SIV-infected rhesus macaques is highly correlated with myocardial viral load. As cardiomyocytes are not productively infected, damage may be an indirect process attributable to a combination of pro-inflammatory mediators and viral proteins.

Methods and Results—Given the diverse roles of CCR5 in mediating recruitment of leukocytes to inflammatory sites and serving as a receptor for HIV entry into cells, we investigated the role of CCR5 in the SIV/macaque model of diastolic dysfunction. We found that in SIV-infected macaques, CCR5 inhibition dramatically impacted myocardial viral load measured by qRT-PCR and prevented diastolic dysfunction measured by echocardiography. Complementary in vitro experiments using fluorescence microscopy showed that CCR5 ligands impaired contractile function of isolated cardiomyocytes, thus identifying CCR5 signaling as a novel mediator of impaired cardiac mechanical function.

Conclusions—Together, these findings incriminate SIV/HIV gp120-CCR5 as well as chemokine-CCR5 interactions in HIV-associated cardiac dysfunction. These findings also have important implications for the treatment of HIV-infected individuals: in addition to antiviral properties and reduced chemokine-mediated recruitment and activation of inflammatory cells, CCR5 inhibition may provide a cardioprotective benefit by preventing cardiomyocyte CCR5 signaling. (*J Am Heart Assoc*. 2014;3:e000874 doi: 10.1161/JAHA.114.000874)

Key Words: animal model • chemokine • diastolic function • echocardiography • HIV

H IV-induced cardiac dysfunction presents a major potential health challenge for over 34 million infected individuals. Although antiretroviral treatment (ART) has reduced the incidence of cardiomyopathy that often accompanies development of AIDS, diastolic dysfunction remains highly prevalent in asymptomatic as well as ART-treated HIV patients.[1–4] Overall cardiac function is depressed in HIV/AIDS but the causes remain obscure. As cardiomyocytes are not productively infected by HIV,[5–9] damage to cardiomyocytes is likely an indirect process that results from a combination of pro-inflammatory mediators and viral proteins.[5–11] Like HIV, productive simian immunodeficiency virus (SIV) infection in the myocardium is localized to macrophages. The SIV/macaque model has facilitated the study of the pathophysiology of HIV-induced cardiac dysfunction, revealing that diastolic dysfunction in SIV-infected rhesus macaques is highly correlated with myocardial viral load.[10,12,13]

The chemokine CCL5 orchestrates recruitment of monocyte/macrophages and resting/effector T cells to inflammatory sites through binding to CCR5.[14] In the heart, treatment with an anti-CCL5 monoclonal antibody significantly reduced macrophage infiltration, infarct size, and post-infarction left ventricular dysfunction in a mouse model of chronic ischemia.[15] As CCR5 also serves as a receptor for HIV entry, CCR5 inhibition blocks HIV infection of cells expressing CCR5 including macrophages in the heart. Given these diverse roles, CCR5 presents an attractive target to block both pro-inflammatory chemokine ligands of CCR5 (CCL3–5) as well as HIV

gp120. In our studies, we evaluated whether treating SIV-infected macaques with the CCR5 inhibitor maraviroc (MVC) prevented diastolic dysfunction as well as whether isolated cardiac ventricular myocytes expressed functional CCR5.

Materials and Methods

In Vivo Studies

Rhesus macaques (*Macaca mulatta*) were inoculated intravenously with the macrophage-tropic clone SIV/17E-Fr and the immunosuppressive swarm SIV/DeltaB670 as previously described and treated with maraviroc (Pfizer, Inc. 200 mg PO BID) beginning 24 days post-inoculation.[16–18] MVC-treated animals were euthanized at a study endpoint 180 days post-inoculation, the mean survival time-point for a cohort of untreated SIV-infected macaques.[10] At euthanasia, all animals were perfused with saline to remove blood and leukocytes from the systemic vasculature. Hearts were immediately harvested and samples were immersion fixed in Streck Tissue Fixative (Streck) or flash frozen. Animal studies were approved by the Johns Hopkins Institutional Animal Care and Use Committee per Animal Welfare Act regulations and the USPHS Policy on Humane Care and Use of Laboratory Animals.

For all studies, cardiac function was evaluated by echocardiography performed by a single sonographer blinded to animal infection and treatment status.[10,19] Prior to inoculation, cardiac function for all animals was evaluated by pulsed-wave Doppler and M-mode echocardiogram in combination with a 2D echocardiogram to record baseline myocardial velocities, wall thickness and chamber dimensions under ketamine anesthesia (5 to 10 mg/kg IM).[10,19] Diastolic function was evaluated by both mitral flow and tissue Doppler echocardiography. Transthoracic echocardiography was performed in the left lateral decubital position using a Sequoia Acuson C256 ultrasound machine equipped with 15 MHz linear transducer and ECG monitor. Data were recorded over 5 cardiac cycles at a sweep speed of 200 mm/s with simultaneous 3-limb lead electrocardiography stored digitally and measured (mean of 3 to 5 values) at the completion of each study. Measurements were performed according to the recommendations set by the American Society of Echocardiography.[19] Each heart was imaged in the 2D mode in the standard parasternal short, parasternal long, 4- and 5-chamber axis views. Mitral inflow and left ventricular outflow velocity-time interval traces were obtained by placing the pulsed Doppler sample probe adjacent to the anterior mitral valve leaflet tip in the left ventricle outflow tract in the apical 4-chamber view. Tissue Doppler imaging (TDI) was used to measure time intervals and myocardial velocities. From the apical 4-chamber view, the sample volume was placed in the ventricular myocardium immediately adjacent to the mitral annulus in either the septal or lateral wall.

Two to 3 pre-inoculation studies were performed on each animal to establish individual baseline values. Echocardiography evaluation was repeated immediately prior to euthanasia. Alterations in cardiac performance were calculated by subtracting terminal measurements from the mean baseline values for MVC-treated rhesus macaques. SIV-infected rhesus macaques treated with MVC were compared with a previously reported cohort of dual-inoculated macaques and uninfected controls.[10] To account for any influence of aging on cardiac function, comparisons were made to either baseline-to-terminal values for untreated macaques surviving ≤180 days, or changes from baseline-to-d180 echo measurement for macaques surviving >180 days.

Immunostaining

To immunophenotype and measure myocardial macrophage populations, single-label indirect immunohistochemistry was performed on Streck-fixed, paraffin-embedded 5 μm sections of myocardium. Antigen retrieval consisted of microwaving heart sections in sodium citrate buffer for 8 minutes. Peroxide block was used on sections to quench endogenous peroxidase activity followed by nonspecific background block (Power Block, Biogenex). Sections were incubated with primary antibody (CD68, 1:2000, clone KP1, DAKO; CD163, 1:10 000, clone Ber-MAC3, AbD Serotec) for 1 hour at room temperature. Sections were then incubated sequentially in biotinylated secondary multilink antibody and horseradish peroxidase-labeled streptavidin or alkaline phosphatase linked (Biogenex) depending on the chromagen with subsequent detection using chromogenic substrate 3,3′-diaminobenzidine or vector red. In the heart, 15 nonoverlapping 200× fields of left ventricular myocardium were captured for analysis; immunostaining for CD68 and CD163 in myocardium was measured by quantitative digital image analysis.[10]

Isolated rhesus ventricular cardiomyocytes VCM were rinsed with ice cold phosphate buffered saline PBS and then fixed with 4% paraformaldehyde (4°C). Fixed cells were rinsed with PBS 0.2% Triton and then incubated with blocking solution (PBS+5% BSA+2% goat serum+0.01% NaN_3+0.2% Triton) for 30 minutes at room temperature. Cells were incubated with anti-CCR5 antibody (BD 3A9, 1:50 in blocking solution) at 4°C overnight. Cells were washed (PBS+Triton 0.2%), incubated in the dark with Alexafluor conjugated secondary antibody (1:200 in blocking solution) for 1 hour at room temperature. After additional washes, cells were washed once with PBS and slides were prepared with Prolong Gold (Life Technologies).

Viral Load Measurements

To evaluate SIV RNA levels, RNA was extracted from frozen left ventricle; plasma virus was pelleted from 140 μL of

plasma. Viral load was measured by qRT-PCR using primers to quantitate SIV gag.[10]

Contraction Measurement and Whole Ca^{2+} Transients in Rhesus Macaque Ventricular Myocytes

Single cell imaging experiments were performed on cardiomyocytes isolated from 9 uninfected rhesus macaques. Hearts collected from uninfected adult rhesus macaques euthanized with intravenous pentobarbital sodium were collagenase digested using a Langendorff apparatus. Via aortic cannula, the hearts were perfused with isolation buffer solution (in mmol/L: 116 NaCl, 26 NaHCO$_3$ 11 NaH$_2$PO$_4$, 1.6 MgSO$_4$·7H$_2$O, 5.4 KCl 5 Na-pyruvate; and glucose, 1 mg/mL) to remove blood from the coronary system followed by enzymatic digestion solution (1.2 U/mL trypsin, 1.2 U/mL collagenase). Following mincing and filtering (100 µm mesh), the cell pellet was promptly resuspended in isolation buffer with 50 µmol/L Ca^{2+}. After the myocytes were separated by gravity, the supernatant was aspirated and myocytes were resuspended in Tyrode's solution (in mmol/L: 140 NaCl, 10 HEPES, 1 MgCl$_2$, 5 KCl; and glucose, 1 mg/mL pH 7.4) with 250 µmol/L Ca^{2+}. The final cell pellet was suspended in 1 mmol/L Ca^{2+}.

Single cell imaging experiments were performed immediately after isolation on cardiomyocytes loaded with the membrane-permeable acetoxymethyl ester of Fura 2 (Fura 2-AM 1 mmol/L with DMSO at room temperature). After allowing for intracellular dye de-esterification, field stimulated (Warner Instruments, 0.5 Hz) cells were imaged at room temperature using an inverted fluorescence microscope (Nikon). Single cell recordings of sarcomeric contraction (measured by real-time Fourier transform) and calcium transients (excitation of Fura-2 fluorescence) were measured using an Ionoptix platform. Myocytes were chosen for study according to previously established criteria.[20,21] Recordings were collected from single cells over time while superinfused with Tyrode's solution 1 mmol/L Ca^{2+}. Isolated VCMs were probed for CCR5 expression using ligands of CCR5 and small molecule inhibitor of CCR5, MVC. Cells were sequentially exposed to recombinant human CCL5 (278-RN, R&D Systems) 100 nmol/L alone and with 500 nmol/L of MVC (NIH/AIDS Reagent). As cells were recorded over time, each cell served as its own control.

Statistical Analysis

SIV-infected rhesus macaques treated with MVC were compared to a previously reported cohort of SIV-inoculated macaques.[10] To determine whether treatment with the CCR5 inhibitor maraviroc altered SIV-induced diastolic dysfunction, the change from baseline to either terminal or d180 measurement (infected macaques surviving >180 days) was compared between untreated SIV and maraviroc-treated SIV-infected groups using the Mann-Whitney test. Similarly, to determine whether maraviroc treatment altered myocardial macrophage immune activation induced by SIV or SIV replication in the myocardium, the amount of immunostaining and SIV RNA in untreated SIV and maraviroc treated SIV groups was compared using the Mann-Whitney test. Isolated cardiomyocyte contraction and whole Ca^{2+} transient data (mean of 20 cell contraction cycles/cell at steady state) were compared using repeated measures analysis of variance followed by individual group comparison by paired Student *t* test. In all analyses, statistical significance was defined as a $P<0.05$.

Results

Cardiac function in MVC-treated, SIV-infected macaques was measured by echocardiography and compared with untreated, SIV-infected macaques. While untreated, SIV-infected macaques developed diastolic dysfunction,[10] cardiac function in MVC-treated, SIV-infected macaques was preserved, closely resembling cardiac function measured in untreated, uninfected control animals (Table 1; Figure 1). Untreated, SIV-infected macaques developed significant prolongations in mitral inflow E wave deceleration time (MV DT) over the course of infection; MVC treatment prevented MV DT prolongation (Figure 1A). MVC treatment also prevented SIV-induced changes in mitral valve isovolumetric relaxation time (MV IVRT; Figure 1B). In addition, a comparison of terminal MV measurements (rather than change over time) showed that most SIV-infected animals (12/22; 54%) had E/A ratios <1 whereas 5 of 6 SIV-infected macaques treated with MVC had E/A ratios >1. Although the difference in terminal E/A ratios between these 2 groups was not statistically significant ($P=0.37$), group sizes in these studies are much smaller than cross-sectional cohort studies of HIV-infected individuals.[3]

Tissue-doppler derived indices of myocardial relaxation were also preserved in MVC treated SIV-infected animals (Figures 1C and 1D). Compared with untreated SIV-infected macaques, lateral myocardial relaxation time (myoRT) and septal myoRT were significantly shorter in MVC-treated animals and were similar to control macaques. SIV-induced alterations in septal E' also were prevented by MVC treatment ($P=0.016$). Given that macaque thoracic anatomy and relatively small heart size (ie, heart weight <50 g) are similar to pediatric patients, the increased accuracy of septal imaging compared to lateral imaging in macaques can be extrapolated from pediatric echocardiography.

In addition to maintaining normal cardiac function, MVC treatment significantly decreased myocardial SIV RNA levels

Table 1. Echocardiographic Assessments of Change in Diastolic Function in Untreated SIV-Infected Macaques Versus Maraviroc-Treated SIV-Infected Macaques

	Control Median (Interquartile Range)	SIV Median (Interquartile Range)	SIV+MVC Median (Interquartile Range)	P Value*
Number of macaques	8	22	6	
Mitral valve				
IVRT, ms	4.50 (−1.81 to 11.61)	8.95 (2.81 to 24.33)	−4.50 (−10.38 to −4.0)	0.0027
DT, ms	0.67 (−13.00 to 15.45)	56.0 (14.67 to 94.3)	−16.5 (−25.50 to 4.25)	0.0013
E, m/s	0.01 (−0.05 to 0.19)	−0.06 (−0.26 to 0.02)	0.03 (−0.04 to 0.22)	0.061
A, m/s	0.04 (−0.13 to 0.20)	0.08 (−0.10 to 0.18)	0.09 (0.00 to 0.23)	0.575
E/A	−0.05 (−0.24 to 0.23)	−0.3 (−0.62 to −0.08)	−0.09 (−0.42 to 0.14)	0.370
TDI septal				
myoRT, ms	4.33 (−0.67 to 7.83)	11.5 (5.08 to 29.15)	−4.50 (−13.37 to 3.00)	0.0019
E', ms	−0.01 (−0.01 to 0.01)	−0.02 (−0.04 to 0.00)	0.01 (0.00 to 0.03)	0.0161
A', m/s	−0.02 (−0.04 to 0.23)	−0.50 (−0.76 to −0.2)	−0.06 (−0.35 to 0.00)	0.2824
E'/A'	−0.19 (−0.40 to 0.23)	−0.50 (−0.76 to −0.2)	−0.06 (−0.35 to 0.00)	0.0310
E/E'	0.81 (0.01 to 1.62)	0.34 (−0.60 to 2.14)	0.82 (−1.69 to 2.11)	0.8011
TDI lateral				
myoRT, ms	3.45 (1.33 to 4.92)	20.67 (5.67 to 36.9)	−4.00 (−8.50 to −1.80)	0.0004
E', ms	0.00 (−0.04 to 0.03)	−0.01 (−0.05 to 0.02)	0.02 (−0.02 to 0.02)	0.2971
A', m/s	0.00 (−0.01 to 0.04)	0.01 (0.00 to 0.04)	0.00 (−0.10 to 0.03)	0.2976
E'/A'	−0.25 (−0.55 to 0.21)	−0.50 (−0.76 to 0.03)	0.28 (−0.42 to 0.65)	0.0468
E/E'	−5.02 (−6.72 to −3.86)	−2.51 (−5.6 to −0.67)	−0.65 (−2.42 to 0.66)	0.1236

Table values are change from baseline calculated by subtracting the baseline mean from the terminal or day 180 PI value. A indicates late diastolic wave; DT, E wave deceleration time; E, early diastolic wave; IVRT, isovolumetric relaxation time; MI, mitral inflow; MVC, maraviroc; myoRT, myocardial relaxation time; SIV, simian immunodeficiency virus; TDI, tissue Doppler imaging.
*P value indicates Mann-Whitney for SIV vs SIV+MVC using Prism 6.

to below the limit of detection by qRT-PCR in 4 of 6 treated macaques (Figure 2A). Plasma viral load in MVC-treated animals was reduced by 1 to 2 logs after MVC treatment (Figure 2B). As expected for antiretroviral monotherapy, reduction of plasma viremia was transient and pronounced differences in viral load were not apparent from day 90 post-infection through terminal time points.

To determine whether MVC treatment altered macrophage subpopulations in the myocardium, populations were characterized by immunohistochemistry and digital image analysis. Expression of CD163, a macrophage marker that co-localizes with SIV proteins in the brain and the heart, was significantly lower in MVC-treated versus untreated SIV-infected macaques (Figures 2C and 3).[11,22] In contrast, MVC treatment did not alter CD68 levels in infected macaques (Figure 2D).

While increased CCR5 mRNA expression has been reported in the failing myocardium, cell-specificity of CCR5 expression in the heart has not been characterized.[23] Given reports that cardiomyocytes express other cytokine and chemokine receptors, we examined cardiomyocytes for CCR5 expression.[8,24] Using double immunostaining for the cardiomyocyte marker sarcomeric actin and CCR5 followed by confocal microscopy, we identified CCR5 on macaque cardiomyocytes (Figures 4A and 4B). To confirm that CCR5 expressed on cardiomyocytes was functional, viable cardiomyocytes were also isolated from adult rhesus hearts for ex vivo studies. Freshly isolated rhesus macaque cardiomyocytes were exposed sequentially to CCL5, then CCL5 in combination with MVC (Figure 4C). The addition of CCL5 to cardiomyocytes (n=18) significantly reduced myocyte contractility, decreasing sarcomeric fractional shortening by 27% compared with basal contraction (Figure 4E). The subsequent addition of MVC, a CCR5-specific inhibitor, reversed the CCL5-induced decrease in myocyte contractility. Interestingly, CCL5-induced changes in contraction were not coupled to alterations in the amplitude of the whole Ca^{2+} transient (data not shown).

In addition to reducing sarcomere contractility, CCL5 altered the kinetics of cardiomyocyte contraction but not relaxation. CCL5 treatment increased the time to peak contraction as compared with basal by 16%, indicating
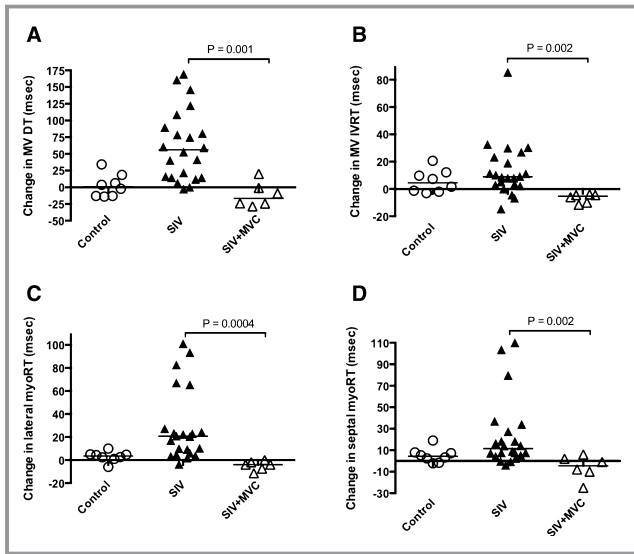
Figure 1. Maraviroc (MVC) therapy preserves diastolic function in SIV-infected macaques. A, MVC-treated SIV-infected macaques had preserved mitral inflow E wave deceleration times (MV DT). B, The median MV isovolumetric relaxation time (IVRT) was also significantly lower with MVC treatment vs untreated SIV-infected macaques. MVC also prevented increases in tissue Doppler (TDI)-derived lateral myocardial relaxation time (myoRT, C) and septal myoRt (D) as compared to untreated SIV-infected macaques. Analyses represent Mann–Whitney tests; bars represent median values. SIV indicates simian immunodeficiency virus.

Figure 2. Maraviroc (MVC) reduces viral replication in heart and plasma, and macrophage activation in myocardium. A, Simian immunodeficiency virus (SIV) RNA levels in the heart were significantly lower in MVC-treated SIV-infected macaques vs untreated SIV-infected macaques. B, Mean plasma viral load over the course of infection in MVC-treated vs untreated SIV-infected macaques showed an initial 1 to 2 log decrease in SIV RNA. C, Total immunostaining for CD163+ macrophages was significantly lower in MVC-treated vs untreated SIV-infected macaques, similar to immunostaining levels in uninfected control macaques (see Figure 3). D, In contrast, MVC treatment did not reduce myocardial immunostaining for CD68 in SIV-infected macaques. Mann-Whitney; bars represent median values.

an impaired cardiomyocyte ability to develop peak tension (Figure 4F). CCL5 did not significantly change myocyte relaxation rate (Figure 4G). However, myocyte relaxation was faster in cardiomyocytes exposed to both CCL5 and MVC as compared with basal relaxation times (Figure 4G).

We then performed a reciprocal experiment in which cardiomyocytes (n=17 cells) were first treated with MVC
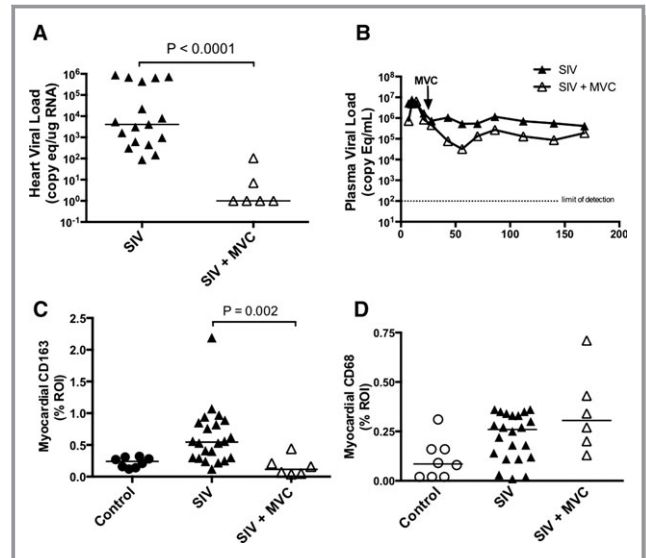
then exposed to a combination of both CCL5 and MVC (Figure 4D). MVC treatment prior to CCL5 addition blocked the previously observed CCL5 effect and did not significantly alter either sarcomere contraction or the whole Ca^{2+} transient. Moreover, MVC treatment alone did not alter the
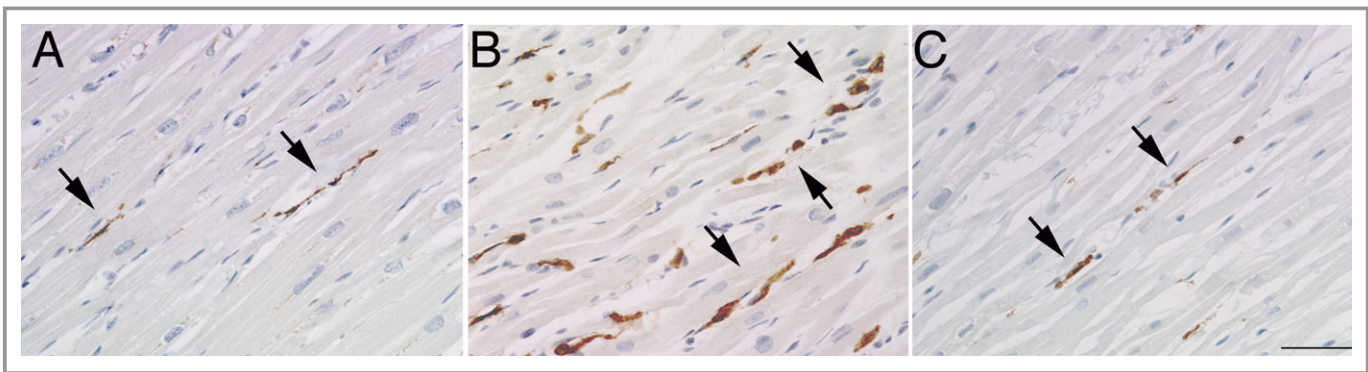

Figure 3. Maraviroc treatment reduced SIV-induced upregulation of macrophage expression of CD163 in myocardium. A, Scattered CD163–immunopositive macrophages (arrow, brown cytoplasm) were present in the myocardium of uninfected control animals. B, The number and cell size of interstitial and perivascular CD163-positive macrophages increased with SIV infection. C, Maraviroc treatment prevented upregulation of CD163 in myocardium of SIV-infected macaques. Bar=100 μM.
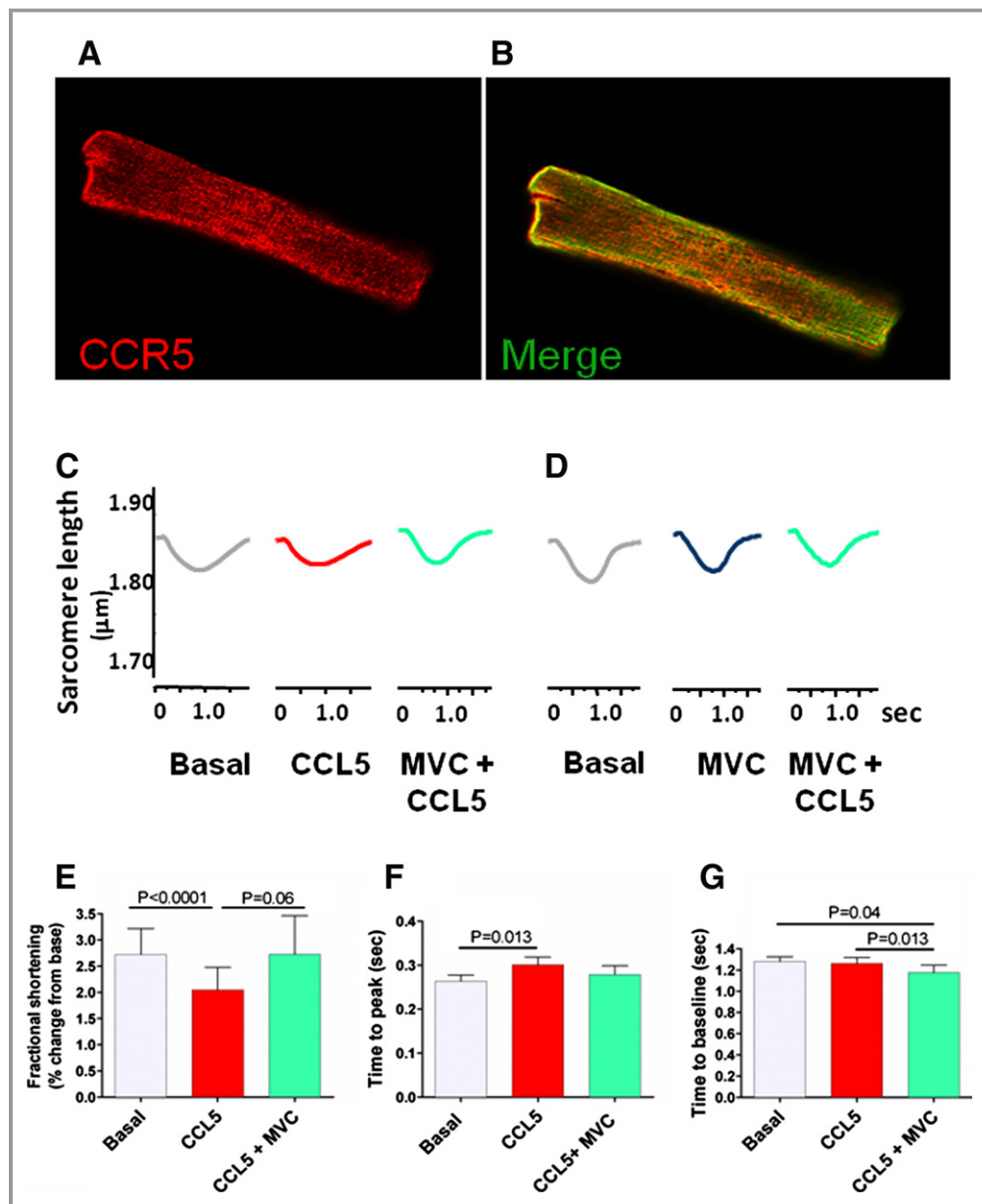
Figure 4. CCL5 decreases cardiomyocyte contractility via CCR5. Confocal microscopy showing expression of (A) CCR5 (red) on isolated adult rhesus macaque ventricular cardiomyocyte (RM VCM) merged with (B) sarcomeric actin (green). C, Representative twitch traces for VCM sequentially exposed to human recombinant CCL5 (100 nmol/L), then CCL5 (100 nmol/L) with maraviroc (MVC, 500 nmol/L). Compared to basal conditions (grey, left), CCL5 decreased contractility, shown by the reduced, flattened twitch amplitude (red, middle). The CCL5-induced decline in contractility was reversed by subsequent addition of MVC with CCL5 (green, right). D, Representative twitch traces for reciprocal experiments showing VCM sequentially exposed to MVC (500 nmol/L) followed by a combination CCL5 (100 nmol/L) and MVC (500 nmol/L). Addition of MVC (blue, middle) did not alter contraction from basal (grey, left). Furthermore, addition of MVC prior to MVC+CCL5 (turquoise, left) prevented CCL5-induced changes in contractility with twitch traces unchanged from basal. E, Summary data for RM VCM exposed to CCL5 (100 nmol/L) followed by MVC (500 nmol/L) with CCL5 (100 nmol/L). CCL5 significantly decreased fractional shortening compared to basal. Subsequent addition of MVC modulated the CCL5 effect towards basal shortening. F, CCL5 significantly increases the time from basal to 50% peak sarcomere length (t to pk) compared to basal conditions. Subsequent CCL5+MVC modulated t to pk shortening towards basal conditions. G, CCL5 did not significantly change the time from peak shortening to 50% baseline (t to bl) compared to basal conditions although t to bl in cells treated with CCL5+MVC was shorter than both basal and CCL5 treatment. Paired *t*-tests, mean value indicated by the top of bar with bars representing standard error.

rate of cardiomyocyte contraction or relaxation (data not shown).

Discussion

The echocardiographic data show that CCR5 inhibition prevented diastolic dysfunction in SIV infection, demonstrating clearly that CCR5 ligands play important roles in cardiac dysfunction. In addition to maintaining normal cardiac function, maraviroc treatment significantly decreased myocardial SIV RNA levels in treated infected macaques. As reduction of plasma viremia was transient, the major sustained impact of MVC treatment on viral replication was in the heart rather than in blood.

Our previous studies found that myocardial macrophage activation was necessary for development of diastolic dysfunction.[10] Expression of CD163, a macrophage marker that co-localizes with SIV protein, was significantly lower in MVC-treated versus untreated SIV-infected macaques while CD68 levels were unchanged. The strong positive correlation we previously found between myocardial expression of CD163 and CD68 in SIV-infected macaques was not maintained in MVC-treated SIV-infected macaques. Together, these data show that the anti-inflammatory impact of MVC treatment is focused on specific macrophage subpopulations in the heart and further suggests an important role for CD163+ macrophages in particular in the development of HIV-induced cardiac dysfunction. Additional studies are necessary to establish the immunomodulatory impact of CCR5 inhibition on myocardial macrophage subpopulations.

Our functional data from isolated viable macaque cardiomyocytes demonstrate that CCL5 binding to CCR5 alters cardiomyocyte mechanical function without inducing alterations in the amplitude of the whole Ca^{2+} transient. CCL5-induced changes in fractional shortening can be reversed or prevented with CCR5 inhibition, demonstrating that MVC treatment can prevent CCR5-mediated cardiomyocyte mechanical dysfunction. The finding that CCL5-induced changes in cardiac cell contractility and relaxation develop in the absence of salient modifications of the whole Ca^{2+} transient suggests that CCL5 binding to CCR5 desensitizes myofilament proteins to the effects produced by physiological levels of intracellular Ca^{2+}. Studies in rodent models have also suggested that HIV gp120 can induce desensitization of myofilaments.[9]

Although HIV and SIV use the chemokine receptor CCR5 to gain entry to susceptible cell types including macrophages infiltrating the myocardium, binding and signaling through chemokine receptors CXCR4 or CCR5 can occur independent of viral entry.[25–27] HIV gp120 signaling through chemokine receptors resembles the action of cognate chemokine ligands, contributing to the deleterious outcomes associated with sustained immune activation. As conformationally appropriate trimeric SIV gp120 is unavailable, we used CCL5 to emulate SIV gp120 binding to cardiomyocyte CCR5. The dramatic impact of MVC treatment on both myocardial viral load and prevention of diastolic dysfunction in SIV-infected macaques implicates SIV gp120-CCR5 as well as chemokine-CCR5 interactions in cardiac dysfunction.

MVC treatment in HIV patients is limited by the requirement to characterize HIV co-receptor usage prior to starting MVC treatment.[28–30] Widespread use of CCR5 antagonists for HIV is further hampered by concerns over drug resistance and emergence of HIV strains utilizing chemokine receptor CXCR4 due to selective pressure. Nonetheless, MVC is unique because, in addition to blocking HIV entry, it has substantial immunomodulatory effects including dampening chemokine signaling that mediates monocyte-macrophage recruitment through CCR5.[31] Our studies show a novel potential beneficial role for CCR5 inhibitors in preserving cardiomyocyte contractility in the face of CCR5 ligands.

As survival of HIV-infected patients increases, additional cardiac insults including aging and coronary artery disease will be superimposed upon primary HIV cardiac damage. The cumulative impact may be profound, highlighting the need for novel therapeutic approaches such as addition of CCR5 inhibitors to prevent early and ongoing cardiac damage. This study revealed 2 major findings: (1) in vivo CCR5 inhibition prevented diastolic dysfunction in SIV-infected macaques and (2) in vitro experiments showed that CCR5 ligands impair contractile function of cardiomyocytes, thus identifying CCR5 signaling as a novel mediator of impaired cardiac mechanical function. Together, these findings illustrate that therapeutic CCR5 inhibition offers multiple advantages for HIV treatment. In addition to antiviral properties and reduced chemokine-mediated recruitment and activation of inflammatory cells, CCR5 inhibition provides an additional cardioprotective benefit by preventing cardiomyocyte CCR5 signaling. In disease settings associated with chronic inflammation, including post-infarction, sustained production of CCR5 ligands can induce CCR5-mediated cardiomyocyte functional impairment, extending the significance of our findings beyond HIV.[15]

Acknowledgments

Sources of Funding

Disclosures

None.

References

1. Barbaro G, Barbarini G, Di Lorenzo G. Early impairment of systolic and diastolic function in asymptomatic HIV-positive patients: a multicenter echocardiographic and echo-Doppler study. The Gruppo Italiano Per Lo Studio Cardiologico dei Pazienti Affetti da AIDS. *AIDS Res Hum Retroviruses*. 1996;12:1559–1563.

2. Longo-Mbenza B, Seghers LV, Vita EK, Tonduangu K, Bayekula M. Assessment of ventricular diastolic function in AIDS patients from Congo: a Doppler echocardiographic study. *Heart*. 1998;80:184–189.

3. Hsue PY, Hunt PW, Ho JE, Farah HH, Schnell A, Hoh R, Martin JN, Deeks SG, Bolger AF. Impact of HIV infection on diastolic function and left ventricular mass. *Circ Heart Fail*. 2010;3:132–139.

4. Schuster I, Thoni GJ, Ederhy S, Walther G, Nottin S, Vinet A, Boccara F, Khireddine M, Girard PM, Mauboussin JM, Rouanet I, Dauzat M, Cohen A, Messner-Pellenc P, Obert P. Subclinical cardiac abnormalities in human immunodeficiency virus-infected men receiving antiretroviral therapy. *Am J Cardiol*. 2008;101:1213–1217.

5. Twu C, Liu NQ, Popik W, Bukrinsky M, Sayre J, Roberts J, Rania S, Bramhandam V, Roos KP, MacLellan WR, Fiala M. Cardiomyocytes undergo apoptosis in human immunodeficiency virus cardiomyopathy through mitochondrion- and death receptor-controlled pathways. *Proc Natl Acad Sci USA*. 2002;99:14386–14391.

6. Kan H, Xie Z, Finkel MS. p38 MAP kinase-mediated negative inotropic effect of HIV gp120 on cardiac myocytes. *Am J Physiol Cell Physiol*. 2004;286:C1–C7.

7. Kan H, Xie Z, Finkel MS. iPLA2 inhibitor blocks negative inotropic effect of HIV gp120 on cardiac myocytes. *J Mol Cell Cardiol*. 2006;40:131–137.

8. Yuan Y, Kan H, Fang Q, Chen F, Finkel MS. CXCR4 receptor antagonist blocks cardiac myocyte p38 MAP kinase phosphorylation by HIV gp120. *Cardiovasc Toxicol*. 2008;8:173–180.

9. Berzingi C, Chen F, Finkel MS. p38 MAP kinase inhibitor prevents diastolic dysfunction in rats following HIV gp120 injection in vivo. *Cardiovasc Toxicol*. 2009;9:142–150.

10. Kelly KM, Tarwater PM, Karper JM, Bedja D, Queen SE, Tunin RS, Adams RJ, Kass DA, Mankowski JL. Diastolic dysfunction is associated with myocardial viral load in simian immunodeficiency virus-infected macaques. *Aids*. 2012;26:815–823.

11. Yearley JH, Pearson C, Shannon RP, Mansfield KG. Phenotypic variation in myocardial macrophage populations suggests a role for macrophage activation in SIV-associated cardiac disease. *AIDS Res Hum Retroviruses*. 2007;23:515–524.

12. Yearley JH, Pearson C, Carville A, Shannon RP, Mansfield KG. SIV-associated myocarditis: viral and cellular correlates of inflammation severity. *AIDS Res Hum Retroviruses*. 2006;22:529–540.

13. Shannon RP. SIV cardiomyopathy in non-human primates. *Trends Cardiovasc Med*. 2001;11:242–246.

14. Schall TJ, Bacon K, Toy KJ, Goeddel DV. Selective attraction of monocytes and T lymphocytes of the memory phenotype by cytokine rantes. *Nature*. 1990;347:669–671.

15. Montecucco F, Braunersreuther V, Lenglet S, Delattre BM, Pelli G, Buatois V, Guilhot F, Galan K, Vuilleumier N, Ferlin W, Fischer N, Vallee JP, Kosco-Vilbois M, Mach F. CC chemokine CCL5 plays a central role impacting infarct size and post-infarction heart failure in mice. *Eur Heart J*. 2012;33:1964–1974.

16. Clements JE, Babas T, Mankowski JL, Suryanarayana K, Piatak M Jr, Tarwater PM, Lifson JD, Zink MC. The central nervous system as a reservoir for simian immunodeficiency virus (SIV): steady-state levels of SIV DNA in brain from acute through asymptomatic infection. *J Infect Dis*. 2002;186:905–913.

17. Zink MC, Amedee AM, Mankowski JL, Craig L, Didier P, Carter DL, Munoz A, Murphey-Corb M, Clements JE. Pathogenesis of SIV encephalitis. Selection and replication of neurovirulent SIV. *Am J Pathol*. 1997;151:793–803.

18. Zink MC, Suryanarayana K, Mankowski JL, Shen A, Piatak M Jr, Spelman JP, Carter DL, Adams RJ, Lifson JD, Clements JE. High viral load in the cerebrospinal fluid and brain correlates with severity of simian immunodeficiency virus encephalitis. *J Virol*. 1999;73:10480–10488.

19. Schiller NB, Shah PM, Crawford M, DeMaria A, Devereux R, Feigenbaum H, Gutgesell H, Reichek N, Sahn D, Schnittger I, Silverman NH, Tajik AJ. Recommendations for quantitation of the left ventricle by two-dimensional echocardiography. American Society of Echocardiography Committee on standards, subcommittee on quantitation of two-dimensional echocardiograms. *J Am Soc Echocardiogr*. 1989;2:358–367.

20. Capogrossi MC, Kort AA, Spurgeon HA, Lakatta EG. Single adult rabbit and rat cardiac myocytes retain the Ca^{2+}- and species-dependent systolic and diastolic contractile properties of intact muscle. *J Gen Physiol*. 1986;88:589–613.

21. Tocchetti CG, Wang W, Froehlich JP, Huke S, Aon MA, Wilson GM, Di Benedetto G, O'Rourke B, Gao WD, Wink DA, Toscano JP, Zaccolo M, Bers DM, Valdivia HH, Cheng H, Kass DA, Paolocci N. Nitroxyl improves cellular heart function by directly enhancing cardiac sarcoplasmic reticulum Ca^{2+} cycling. *Circ Res*. 2007;100:96–104.

22. Kim WK, Alvarez X, Fisher J, Bronfin B, Westmoreland S, McLaurin J, Williams K. CD163 identifies perivascular macrophages in normal and viral encephalitic brains and potential precursors to perivascular macrophages in blood. *Am J Pathol*. 2006;168:822–834.

23. Damas JK, Eiken HG, Oie E, Bjerkeli V, Yndestad A, Ueland T, Tonnessen T, Geiran OR, Aass H, Simonsen S, Christensen G, Froland SS, Attramadal H, Gullestad L, Aukrust P. Myocardial expression of CC- and CXC-chemokines and their receptors in human end-stage heart failure. *Cardiovasc Res*. 2000;47:778–787.

24. Pyo RT, Sui J, Dhume A, Palomeque J, Blaxall BC, Diaz G, Tunstead J, Logothetis DE, Hajjar RJ, Schecter AD. CXCR4 modulates contractility in adult cardiac myocytes. *J Mol Cell Cardiol*. 2006;41:834–844.

25. Kaul M, Ma Q, Medders KE, Desai MK, Lipton SA. HIV-1 coreceptors CCR5 and CXCR4 both mediate neuronal cell death but CCR5 paradoxically can also contribute to protection. *Cell Death Differ*. 2007;14:296–305.

26. Medders KE, Sejbuk NE, Maung R, Desai MK, Kaul M. Activation of p38 mapk is required in monocytic and neuronal cells for HIV glycoprotein 120-induced neurotoxicity. *J Immunol*. 2010;185:4883–4895.

27. Klein RS, Williams KC, Alvarez-Hernandez X, Westmoreland S, Force T, Lackner AA, Luster AD. Chemokine receptor expression and signaling in macaque and human fetal neurons and astrocytes: implications for the neuropathogenesis of AIDS. *J Immunol*. 1999;163:1636–1646.

28. Troia-Cancio P, Asmuth DM. Lessons from maraviroc clinical trials. *Expert Rev Anti Infect Ther*. 2011;9:649–651.

29. Wasmuth JC, Rockstroh JK, Hardy WD. Drug safety evaluation of maraviroc for the treatment of HIV infection. *Expert Opin Drug Saf*. 2012;11:161–174.

30. Gulick RM, Lalezari J, Goodrich J, Clumeck N, DeJesus E, Horban A, Nadler J, Clotet B, Karlsson A, Wohlfeiler M, Montana JB, McHale M, Sullivan J, Ridgway C, Felstead S, Dunne MW, van der Ryst E, Mayer H. Maraviroc for previously treated patients with r5 HIV-1 infection. *N Engl J Med*. 2008;359:1429–1441.

31. Rossi R, Lichtner M, De Rosa A, Sauzullo I, Mengoni F, Massetti AP, Mastroianni CM, Vullo V. In vitro effect of anti-human immunodeficiency virus CCR5 antagonist maraviroc on chemotactic activity of monocytes, macrophages and dendritic cells. *Clin Exp Immunol*. 2011;166:184–190.